AFRL-AFOSR-VA-TR-2021-0084

Toward Electrically-Pumped Lasing in Organic-Inorganic Hybrid Perovskite Semiconductors

Giebink, Noel
PENNSYLVANIA STATE UNIVERSITY
201 OLD MAIN
UNIVERSITY PARK, PA,
US

07/27/2021
Final Technical Report

Air Force Research Laboratory
Air Force Office of Scientific Research
Arlington, Virginia 22203
Air Force Materiel Command

REPORT DOCUMENTATION PAGE

Form Approved
OMB No. 0704-0188

1. REPORT DATE *(DD-MM-YYYY)*	**2. REPORT TYPE**	**3. DATES COVERED** *(From - To)*
27-07-2021	Final	01 May 2018 - 30 Apr 2021

4. TITLE AND SUBTITLE
Toward Electrically-Pumped Lasing in Organic-Inorganic Hybrid Perovskite Semiconductors

5a. CONTRACT NUMBER

5b. GRANT NUMBER
FA9550-18-1-0037

5c. PROGRAM ELEMENT NUMBER
61102F

6. AUTHOR(S)
Noel Giebink

5d. PROJECT NUMBER

5e. TASK NUMBER

5f. WORK UNIT NUMBER

7. PERFORMING ORGANIZATION NAME(S) AND ADDRESS(ES)
PENNSYLVANIA STATE UNIVERSITY
201 OLD MAIN
UNIVERSITY PARK, PA
US

8. PERFORMING ORGANIZATION REPORT NUMBER

9. SPONSORING/MONITORING AGENCY NAME(S) AND ADDRESS(ES)
AF Office of Scientific Research
875 N. Randolph St. Room 3112
Arlington, VA 22203

10. SPONSOR/MONITOR'S ACRONYM(S)
AFRL/AFOSR RTB2

11. SPONSOR/MONITOR'S REPORT NUMBER(S)
AFRL-AFOSR-VA-TR-2021-0084

12. DISTRIBUTION/AVAILABILITY STATEMENT
A Distribution Unlimited: PB Public Release

13. SUPPLEMENTARY NOTES

14. ABSTRACT
The objective of this program is to establish the scientific basis needed to realize a hybrid perovskite laser diode. The past year focused on understanding the operation of perovskite light-emitting diodes at extreme current density. We have found that, under short (<50 ns) pulses with suitable thermal management, that we can achieve 1-5 kA/cm2 current densities while maintaining external quantum efficiencies >1%. This result is significant because it implies electrically-injected excitation density nearing what we know achieves lasing under optical excitation. In parallel with this development, we also developed an analytical model for ideal organic and perovskite laser diodes based on the argument that their intrinsic active layers necessitate operation in the bipolar space charge-limited current regime. We obtained rigorous analytical expressions for the threshold voltage and current density and identified fundamental limits for laser operation in the presence of parasitic annihilation and excited state absorption losses that should serve to guide the future of organic laser diode technology. We published 4 manuscripts in this reporting period, with 1 more in preparation and 1 provisional patent filing. Owing to a COVID-related delay in spending over the past year, we obtained a no cost extension to complete the objectives of this program and expect to achieve electrically-pumped lasing in the coming year.

15. SUBJECT TERMS

16. SECURITY CLASSIFICATION OF:			**17. LIMITATION OF ABSTRACT**	**18. NUMBER OF PAGES**	**19a. NAME OF RESPONSIBLE PERSON**
a. REPORT	**b. ABSTRACT**	**c. THIS PAGE**			KENNETH CASTER
U	U	U	UU	9	**19b. TELEPHONE NUMBER** *(Include area code)* 0000 0000

AFOSR YIP Annual Performance Report

Reporting period: 5/1/20 – 4/30/21

Grant #: FA9550-18-1-0037
Program: Organic Materials Chemistry
Program Manager: Dr. Kenneth Caster
Institutions: Penn State and Princeton University
Project PIs: Chris Giebink and Barry Rand

Toward electrically-pumped lasing in hybrid organic-inorganic perovskite semiconductors

I. Executive Summary

The objective of this program is to establish the scientific basis needed to realize a hybrid perovskite laser diode. The past year focused on understanding the operation of perovskite light-emitting diodes at extreme current density. We have found that, under short (<50 ns) pulses with suitable thermal management, that we can achieve 1-5 kA/cm^2 current densities while maintaining external quantum efficiencies >1%. This result is significant because it implies electrically-injected excitation density nearing what we know achieves lasing under optical excitation. In parallel with this development, we also developed an analytical model for ideal organic and perovskite laser diodes based on the argument that their intrinsic active layers necessitate operation in the bipolar space charge-limited current regime. We obtained rigorous analytical expressions for the threshold voltage and current density and identified fundamental limits for laser operation in the presence of parasitic annihilation and excited state absorption losses that should serve to guide the future of organic laser diode technology. We published 4 manuscripts in this reporting period, with 1 more in preparation and 1 provisional patent filing. Owing to a COVID-related delay in spending over the past year, we obtained a no cost extension to complete the objectives of this program and expect to achieve electrically-pumped lasing in the coming year.

II. Research Summary

Perovskites diodes under extreme current density. To reduce parasitic capacitance that we experienced in previously reported devices, and in an effort to be able to probe intrinsic, material-related speed limitations for perovskite LEDs (PeLEDs), we employed a device configuration as shown in Figure 1a. Rather than a patterned insulating layer to define device area, the device area is defined by the overlap between a narrow ITO anode strip (200 μm) and a narrow Ag cathode strip (150 μm). To reduce series resistance, the narrow indium tin oxide (ITO) anode strip is connected to millimeter-wide Au contacts and the narrow Ag cathode strip is connected to millimeter-wide Ag contacts. Using this configuration, PeLED operation speed is dramatically improved. Figure 1b-d shows the electroluminescence (EL) response of PeLEDs driven by 5 – 40 ns electrical pulses at current densities from 0.5 kA/cm^2 to 2 kA/cm^2. The EL rise time (defined as the interval between the 10% and 90% amplitude points on the leading edge of a pulse) is reduced from 14.8 ns driven by 0.5 kA/cm^2 to 2.0 ns driven by 2.5 kA/cm^2. Notably, the PeLED is fully

turned on using electrical pulses as short as 5 ns for current densities ≥ 1 kA/cm^2 (Figure 1c).

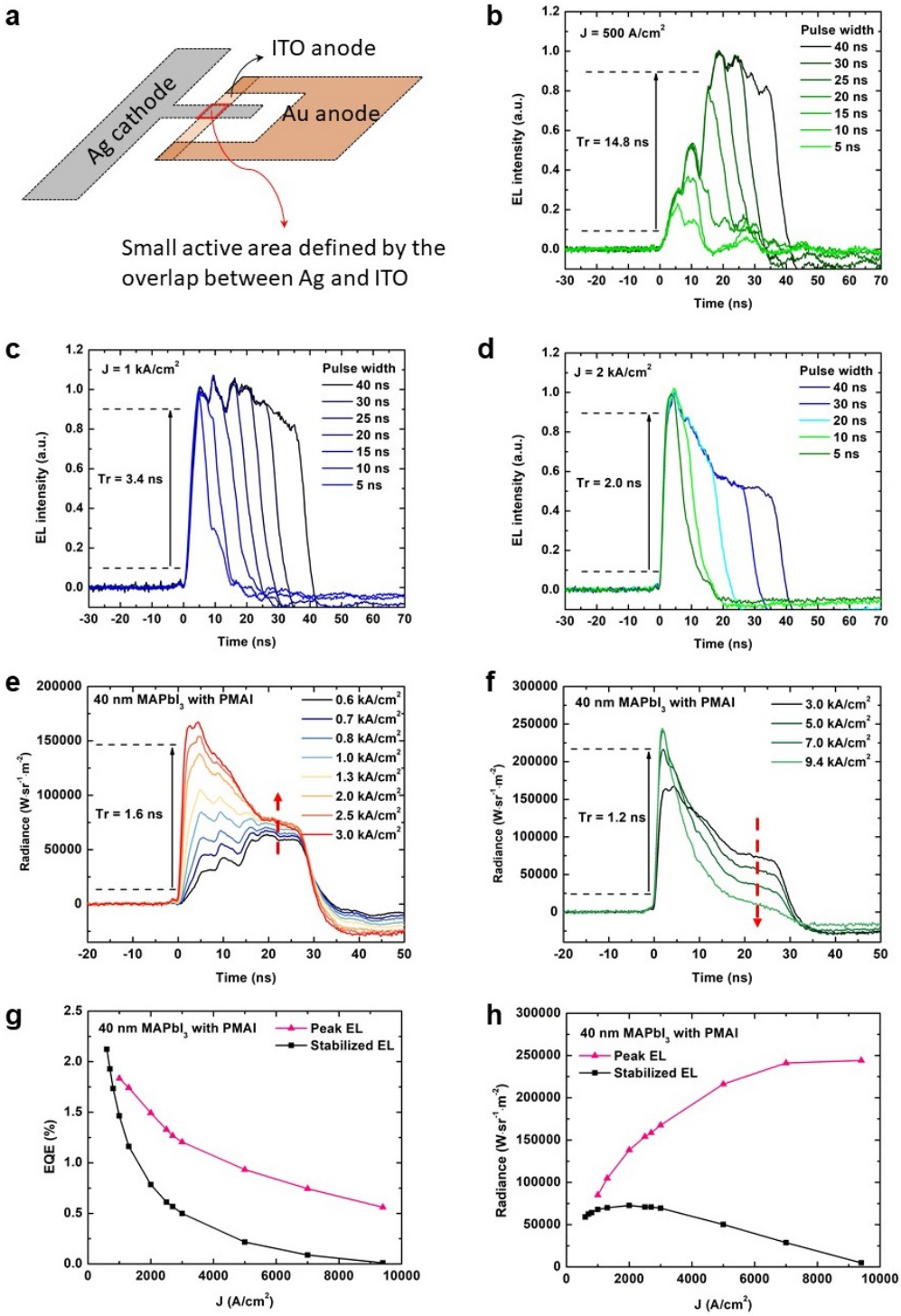

Figure 1. a, Schematic diagram of the device configuration with reduced parasitic capacitance and resistance. **b-d**, EL intensity–time curves for PeLEDs driven by 500 A/cm^2 pulses (**b**), 1 kA/cm^2 pulses (**c**), 2 kA/cm^2 pulses (**d**), with pulsing widths in the range of 5 – 40 ns. **e-f**, Radiance–time curves for PeLEDs driven at various current densities J below 3 kA/cm^2 (**e**) and above 3 kA/cm^2 (**f**). **g-h**, EQE–J curves (**g**) and radiance–J curves (**h**) of PeLEDs driven in pulsed mode.

In Figure 1d, we observe a decrease in EL intensity after the initial peak, which is stabilized after approximately 20 ns. To study this phenomenon in detail, we plot the EL response of 30 ns electrical pulses at various current densities from 0.6 to 9.4 kA/cm^2 in Figure 1e-f, where it can be seen that the EL rise time is further reduced to 1.2 ns when driven with 9.4 kA/cm^2 pulses. Given the approximately 1 ns rise time of the electrical pulse, we suspect that an even shorter EL rise time could be achieved with a faster electrical pulsing source. Below 1 kA/cm^2, a relatively slow EL rise time is observed, with no EL decrease during the entire pulse duration (Figure 1e). Above 1 kA/cm^2, in contrast, a fast initial EL burst is followed by a stabilized EL intensity after approximately 20 ns at a value below the initial peak. The stabilized EL intensity increases with increasing current density until approximately 3 kA/cm^2 (Figure 1e). Above 3 kA/cm^2, the peak EL intensity increases while the stabilized EL intensity decreases as current density increases (Figure 1f), which indicates additional EL quenching pathways are involved at longer time scales. To the best of our knowledge, this is the first time that transient EL dynamics of PeLEDs with nanosecond resolution have been observed. Notably, when the peak EL intensity is considered, rather than the steady-state EL intensity (in practice this can be achieved by shortening the pulsing width as in Figure 1d), considerably reduced EQE roll-off and significantly higher radiance are achieved (Figure 1g-h); EQE of approximately 0.56% and radiance of 244 $\mathrm{kW \cdot sr^{-1} \cdot m^{-2}}$ are achieved at a current density of 9.4 kA/cm^2. In contrast, the steady-state EQE drops to approximately 0.01% and the radiance drops to 4.8 $\mathrm{kW \cdot sr^{-1} \cdot m^{-2}}$ at 9.4 kA/cm^2 due to additional EL quenching pathways involved. The more than 50-fold improvement in peak radiance indicates the importance of short electrical pulses in mitigating the nonradiative charge-carrier recombination losses that are significant at longer time scales.

Analytical model for ideal organic and hybrid perovskite laser diodes. The pandemic-related lab closure this past year also motivated some deeper thought about the way in which organic and perovskite laser diodes have to operate. We realized that, because organic laser have to have an intrinsic gain layer (electrical doping severely quenches excitons), the current-voltage relationship of an ideal laser diode necessarily takes place in the bipolar space charge limited current (SCLC) regime. Making this connection is significant because the bipolar SCLC regime has an analytical solution and therefore we were able to use it to provide the first full analytical description of the threshold condition in an ideal organic laser diode.

Skipping the details of the derivation (which can be found in our published paper Grede *et al.* PRB, 103, L121301 (2021)), the threshold current density and voltage for an ideal organic laser diode are:

$$J_{th} = \frac{qL\alpha k_s}{\chi_s \Gamma \sigma_{st}}$$

and

$$V_{th} = \frac{\pi L^2}{4}\sqrt{\frac{q\alpha k_s}{\chi_s \Gamma \sigma_{st}}} + V_{bi}$$

where q is the electronic charge, L is the active layer thickness, μ is the charge carrier mobility, ε is the dielectric constant, α is the optical mode loss, Γ is the modal confinement factor, σ_{st} is the stimulated emission cross-section, k_s is the radiative rate, χ_s is the singlet spin fraction, and V_{bi} is the built-in potential of the diode. Taking parameter values typical of the 4,4′-bis[(N-carbazole)styryl]bi-phenyl (BSBCz) diode lasers reported by Adachi's group: threshold excitation density of 2x10^{16} cm^{-3}, $k_s = 1$ ns^{-1}, $\varepsilon = 4\varepsilon_0$, $\mu = 10^{-3}$ cm^{2}V^{-1}s^{-1}, 2.7 eV optical gap, and $L = 150$ nm, we obtain $J_{th} = 190$ A/cm^2, $V_{th} = 26$ V, and a threshold power density of 5.1 kW/cm^2 as lower bounds for laser operation. For comparison, the experimentally-recorded values are $J_{th} = 600$ A/cm^2, $V_{th} = 34$ V, and a threshold power density of 20 kW/cm^2.

The equations above highlight the importance of active layer thickness for organic laser diodes. Whereas J_{th} depends weakly on L since $\Gamma \propto L$ to first order, the threshold voltage and power density both scale as $L^{3/2}$. The is important in the context of thermal management because organic laser diodes not only generate more heat than their inorganic counterparts (due to their higher voltage), but have more difficulty dissipating it (due to their lower thermal conductivity) and are less able to withstand high temperature without degrading. Electric field strength, which scales as $L^{1/2}$, is another concern since its maximum in the example above (E_{max} = 2 MV/cm) is comparable to the ~3 MV/cm breakdown field of many organic semiconductors.

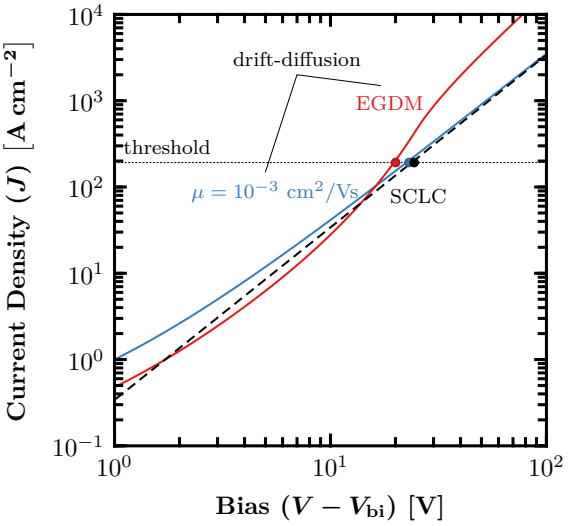

Figure 2. Drift-diffusion simulations of the current-voltage relationship for a BSBCz-like active layer with Ohmic majority carrier injection and equal electron and hole mobilities that are either constant (blue line) or given by the EGDM for disordered organic semiconductors (red). The black dashed line shows the analytical SCL current prediction and solid circles denote the lasing threshold in each case.

Given that the threshold relations above neglect the existence of charge transport layers and also assume infinite carrier densities at the active layer interfaces, it is important to test the accuracy of these results against full drift-diffusion modeling of a real device architecture. Retaining the BSBCz parameters from above, we treat the case of an organic laser with a 150-nm-thick intrinsic active layer and fix the majority carrier concentrations at each edge to 2.5×10^{19} cm^{-3} to simulate Ohmic injection from heavily doped transport layers. Drift-diffusion simulations are carried out using the commercial software SETFOS and the results are presented in Fig. 2 for the case of a constant mobility (10^{-3} cm^2/V s for both electrons and holes; blue) and for the case in which it depends locally on electric field and carrier density according to the extended Gaussian disorder model

(EGDM, red). The threshold current density in both simulations is in good agreement with the analytical prediction; however, the threshold voltage in the EGDM case is slightly lower. This, along with the added current at high bias, is due to the increase in mobility with field and carrier concentration in the EGDM model, which highlights the importance of using mobility values that are congruent with the conditions at threshold.

To sustain the electron and hole concentrations in the middle of the device (and thus the *np* product everywhere), the majority carrier concentrations injected at the active layer edges must be roughly an order of magnitude higher. This is important because it sets the minimum doping concentration required for the transport layers in a laser diode (i.e., due to continuity of *n* and *p*) which, notably, is within the range typical for *p-i-n* OLEDs.

It is also important to assess the impact of triplet exciton and polaron-related optical losses (due to respective absorption cross sections σ_{TT} and σ_{pp} at the lasing wavelength) and quenching interactions (with respective annihilation rate coefficients k_{sta} and k_{spa}). Because the latter typically depend on the former through Förster energy transfer, absorption and annihilation losses must be treated on equal footing. Assuming only one species of polaron (holes in this case) is detrimental, we can incorporate both loss processes in the threshold derivation to obtain J_{th} in the form of an implicit quartic equation:

$$J_{th} = \frac{qL\alpha k_s}{\chi_s \Gamma \sigma_{st}} \left(1 + \frac{J_{th}\chi_T t_{rise} k_{sta}}{qLk_s} + \frac{k_{spa}}{k_s}\sqrt{\frac{\varepsilon J_{th}}{2q^2 L\mu}}\right)\left(1 + \frac{J_{th}\chi_T t_{rise}\sigma_{TT}\Gamma}{qL\alpha} + \frac{\pi\sigma_{pp}\Gamma}{2\alpha}\sqrt{\frac{\varepsilon J_{th}}{2q^2 L\mu}}\right).$$

In this expression, the rise time (t_{rise}) is important because it determines the extent to which long-lived triplet excitons accumulate before the full current density is achieved. Although t_{rise} is nominally characteristic of the electrical pulse, it cannot be significantly faster than the transit time of charge carriers drifting across the active layer since this is the time it takes to establish the SCL recombination profile to begin with (~10 ns for the BSBCz example above).

The form of the equation above is useful because it allows the impact of each loss mechanism to be understood individually. For example, singlet-triplet annihilation on its own doubles the threshold when the middle term in the first set of parentheses is equal to unity. More generally, for this equation to have *any* physically meaningful solution, the absorption and annihilation coefficients must satisfy the following inequalities:

$$\sqrt{\frac{\sigma_{TT}}{\sigma_{st}}} + \sqrt{\frac{\alpha k_{sta}}{\Gamma \sigma_{st} k_s}} < \sqrt{\frac{\chi_s}{\chi_T k_s t_{rise}}}$$

and

$$k_{spa}\sigma_{pp} < \frac{4q\mu\chi_s\sigma_{st}}{\pi\varepsilon}.$$

Figures 3(a) and 3(b) plot these bounds for triplet and polaron losses, respectively, along with contours that show the relative increase in threshold caused by each species. Figure 3(b) also includes the results from full numerical modeling (solid symbols) of the polaron case, validating the approximations used in deriving the equation above.

These results highlight the difference between triplet losses, where a small increase in absorption cross-section or annihilation coefficient can mean the difference between a modest threshold increase and prevention of lasing outright, and polaron losses, where the penalty is more gradual and does not depend on external factors like α or t_{rise}. A blunt way of characterizing this difference is that triplet excitons are either insignificant or catastrophic, whereas the region of parameter space between these extremes is broader for polarons. This highlights the importance of designing new organic gain media like BSBCz that have low overlap between their emission and triplet-triplet absorption spectra, and of implementing device architectures that can deliver high-speed electrical pulses, since this is the difference between success and failure for the classic tris-(8-hydroxyquinoline) aluminum(Alq_3):4-(dicyanomethylene)-2-methyl-6-(4-dimethylamino-styryl)-4*H*-pyran (DCM) gain medium in Fig. 3(a).

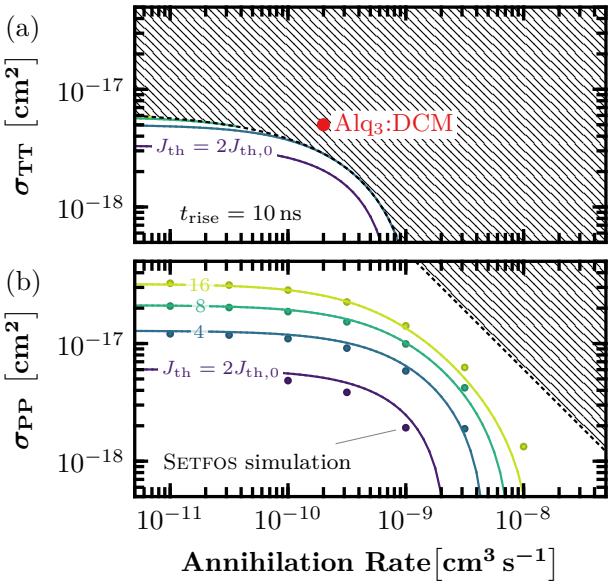

Figure 3. Contours showing the relative increase in threshold cur- rent due to parasitic absorption and singlet exciton annihilation caused by (a) triplet excitons and (b) hole polarons. Lasing is for- bidden in the shaded region at any current density. The solid lines are calculated using the implicit equation and are compared in (b) with the results of the SETFOS numerical modeling (solid circles). The Alq$_3$:DCM material system marked by the red dot in (a) lies in the forbidden region for the t_{rise} = 10 ns case shown.

Another intuitive, but important guideline is to seek organic gain media with equal (and maximal) electron and hole mobilities. To the extent that perfect charge balance is maintained and the envelope of the lasing mode varies negligibly over the active layer, the general solution is largely unaffected when the mobility of one carrier dominates. The problem with imbalanced mobility, however, is that it concentrates recombination toward the lower mobility carrier side of the active layer. This not only exacerbates annihilation loss, but also makes it more challenging to maintain charge balance since the less mobile carrier must be injected at higher density to sustain the same total recombination rate in a narrower region of space.

Finally, we explored whether the same reasoning is also applicable to metal halide perovskite lasers. Though SCLC is less well-studied in this material class, our observations at high current density above and the fact that MHP light emitting diodes use undoped active layers makes it plausible that a perovskite laser diode will operate in the bipolar SCLC regime with free carrier (as opposed to excitonic) gain. Working out this solution, however, we find that because recombination tends to be sub-Langevin (i.e., the bimolecular recombination coefficient is substantially smaller than the Langevin rate), the bipolar SCL current takes place in the injected plasma regime where $n \approx p$ everywhere. Unfortunately, the analytical solution in this limit can greatly overestimate the threshold current because diffusion strongly modifies the *np* product (and thus the recombination

current) near the active layer edges and therefore a full drift-diffusion model is required to accurately describe perovskite lasers.

Overall, these results emphasize a shift in strategy for organic laser diodes from OLED-like architectures characterized by many heterojunctions, blocking layers, and so forth, to a *p*-*i*-*n* structure based on a single, low threshold material that can be degenerately *p*- and *n*-doped, and that has no triplet or polaron absorption overlapping with its emission. With rational design of organic laser materials now emerging to meet these criteria and device architectures guided by the theory above, the path to organic and perovskite laser diodes is coming into clearer focus.

III. Progress on stated objectives

Four primary objectives were set out for this program. These are listed individually below along with their approximate progress toward completion.

Thrust 1: CW optically-pumped lasing. Determine the cause of lasing death in Pv lasers under continuous optical pumping and why it is possible in photoinduced mixed-phase Pv systems at low temperature.

>>Progress: Completed.

Thrust 2: Electrical transport and photophysics under high level injection. Demonstrate current densities >1 kA/cm^2 in Pv thin films and understand the electrical transport regime under high-level injection as well as the origin of quantum efficiency roll-off in Pv LEDs at high brightness.

>>Progress: Complete.

Thrust 3: Electrical doping and charge carrier confinement. Develop doping strategies to increase Pv conductivity with high conductivity transport/blocking layers to maintain charge balance at high current density.

>>Progress: 50% complete.

Thrust 4: Toward electrically-pumped lasing. Demonstrate optically-pumped lasing from a laser diode architecture followed by stimulated emission from Pv semiconductors under electrical pumping and ultimately a Pv laser diode.

>>Progress: 80% complete.

IV. Plans for the coming year

We plan to study high current injection in perovskite laser devices at low temperature in order to decrease their threshold carrier density. From our low temperature optical experiments carried out earlier in this program, we expect to be able to achieve roughly an order of magnitude decrease in the threshold carrier density at low temperature. This, combined with improvements in the laser architecture based on rigorous coupled wave analysis modeling, should put us firmly in the regime where electrically-pumped stimulated emission can be achieved. If we can maintain the same current and quantum

efficiency as above while at low temperature, we therefore have a good chance of achieving the overall program objective and delivering a hybrid perovskite laser diode.

V. Management and financial status

This program is supporting one graduate student at Penn State and one graduate student at Princeton. Spending for this project is summarized in the table below:

Year	Budget outlay	Spending
Y1	$250,000	completely spent
Y2	$250,000	completely spent
Y3	$250,000	~$150,000 (spending delayed by COVID)
Y4 (NCE)	$100,000	

VI. Direct and related publications and patents resulting from this program

Publications:

(During this reporting period)

1. A.J. Grede and N.C. Giebink, "Lasing in the space charge-limited current regime", *Phys. Rev. B*, **103**, L121301 (2021)
2. L. Zhao, K. Roh, S. Kacmoli, K. Al Kurdi, S. Jhulki, S. Barlow, S.R. Marder, C. Gmachl, B.P. Rand, "Thermal management enables bright and stable perovskite light-emitting diodes," *Adv. Mater*., **32**, 2000752 (2020)
3. A. Sridharan, N.K. Noel, B.P. Rand, S. Kéna-Cohen, "Role of photon recycling and band filling in halide perovskite photoluminescence under focused excitation conditions," *J. Phys. Chem. C*, **125**, 2240 (2021)
4. W.B. Gunnarsson and B.P. Rand, "Electrically driven lasing in metal halide perovskites: Challenges and outlook," *APL Mater*., **8**, 030902 (2020).

(During prior reporting periods)

5. H. Kim, J.P. Murphy, L. Zhao, K. Roh, B.P. Rand, and N.C. Giebink, "Optically-pumped lasing from a hybrid perovskite light emitting diode", *Adv. Opt. Mater.* **8**, 1901514 (2020)
6. H. Kim, K. Roh, J.P. Murphy, L. Zhao, W.B. Gunnarsson, E. Longhi, S. Barlow, S.R. Marder, B.P. Rand, and N.C. Giebink, "Factors that limit continuous-wave lasing in hybrid perovskite semiconductors", *Adv. Opt. Mater.* **8**, 1901297 (2020)
7. K. Roh, L. Zhao, W.B. Gunnarsson, Z. Xiao, Y. Jia, N.C. Giebink and B.P. Rand, "Widely tunable, room temperature, single-mode lasing operation from mixed-halide perovskite thin films," *ACS Photonics*, **6**, 3331 (2019).
8. M. Anaya, B.P. Rand, R.J. Holmes, D. Credgington, H.J. Bolink, R.H. Friend, J. Wang, N.C. Greenham and S.D. Stranks, "Best practices for measuring emerging light-emitting diode technologies," *Nat. Photon*., **13**, 818 (2019).
9. N.K. Noel, S.N. Habisreutinger, A. Pellaroque, F. Pulvirenti, B. Wenger, F. Zhang, Y.-H. Lin, O.G. Reid, J. Leisen, Y. Zhang, S. Barlow, S.R. Marder, A.

Kahn, H.J. Snaith, C.B. Arnold, B.P. Rand, "Interfacial charge-transfer doping of metal halide perovskites for high performance photovoltaics," *Energy Environ. Sci.*, **12**, 3063 (2019).
10. S. Jeon, L. Zhao, Y.-J. Jung, J.W. Kim, S.-Y. Kim, H. Kang, J.-H. Jeong, B.P. Rand, J.-H. Lee, "Perovskite light-emitting diodes with improved outcoupling using a high-index contrast nanoarray," *Small*, **15**, 1900135 (2019).
11. Z. Xiao, R.A. Kerner, N. Tran, L. Zhao, G.D. Scholes, B.P. Rand, "Engineering perovskite nanocrystal surface termination for light emitting diodes with external quantum efficiency exceeding 15%," *Adv. Funct. Mater.*, **29**, 1807284 (2019).
12. W. Qiu, Z. Xiao, K. Roh, N.K. Noel, A. Shapiro, P. Heremans, B.P. Rand, "Mixed lead-tin halide perovskites for efficient and wavelength-tunable near-infrared light-emitting diodes," *Adv. Mater.*, **31**, 1806105 (2019).
13. L. Zhao, K.M. Lee, K. Roh, S.-U.-Z. Khan, B.P. Rand, "Improved outcoupling efficiency and stability of perovskite light emitting diodes using thin emitting layers," *Adv. Mater.*, **31**, 1805836 (2019).
14. H. Kim, L. Zhao, J.S. Price, A.J. Grede, K. Roh, A.N. Brigeman, M. Lopez, B.P. Rand, and N.C. Giebink, "Hybrid perovskite light emitting diodes under intense electrical excitation", *Nat. Comm*. **9**, 4893 (2018)

Patents:

(During this reporting period)

1. "Thermal management for perovskite electronic devices" USPTO Provisional Application 63/006,792 filed April 8, 2020.

(During prior periods)

2. "Interdigitated electrode organic and halide perovskite light emitting diodes and lasers" Disclosure filed w/ PSU Tech Transfer Office, 1/25/20.